Development and Evaluation of Ice-/Mixed-Phase Precipitation Models for GPM Radar-Radiometer Algorithm Applications

William Olson[1], Kwo-Sen Kuo[2,4], Lin Tian[3], Mircea Grecu[3], Benjamin Johnson[1], S. Joseph Munchak[4], and Andy Heymsfield[5]

1: Joint Center for Earth Systems Technology/Univ. Maryland Baltimore County; 2: Caelum Research Corporation; 3: Goddard Earth Sciences Technology and Research/Morgan State University; 4: Earth System Science Interdisciplinary Center/Univ. Maryland College Park; 5: National Center for Atmospheric Research

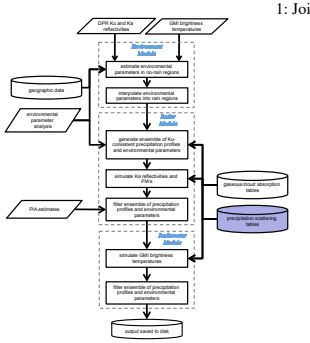

Why? **to improve the physical / statistical models used in GPM radar and combined radar-radiometer precipitation retrieval algorithms.** At left is a schematic of the prototype GPM combined radar-radiometer precipitation estimation algorithm. This algorithm uses input radar reflectivities from the Dual-frequency Precipitation Radar (DPR) and microwave radiances from the GPM Microwave Imager (GMI) to deduce profiles of precipitation in all phases (liquid, ice, and mixed-phase). The accuracy of these precipitation estimates depends not only on the validity of the input data, but also on the realism and representativeness of the physical profile models used to fit the input data.

In the figure at left, the microwave electromagnetic scattering properties of precipitation particles are tabulated in the purple static file. These tabulated scattering properties are functions of the assumed particle phase (temperature), size distribution, density distribution (for ice and mixed-phase), habit, and meltwater fraction. In addition to the tabulated scattering properties, for algorithm applications it is also important to prescribe the statistical behavior of precipitation particle size distributions; e.g., the covariance of particle size distribution parameters as a function of altitude. In sum, the objective of this work is to develop better parameterizations of the physical and statistical properties of ice and mixed-phase precipitation for algorithm applications.

Modeling of Ice/Mixed-Phase Precipitation in Algorithms

Descriptions of the vertical profiles of cloud, precipitation, atmospheric gases, temperature and pressure are needed to compute the profiles of bulk single-scattering properties of atmospheric layers and ultimately, the radar reflectivities and upwelling microwave radiances associated with those profiles. A complete description of all of the atmospheric properties in a vertical column is called a "vertical profile model", and a schematic of such a model suitable for combined radar-radiometer algorithm applications is shown at right, with atmospheric properties specified in each range gate of the DPR.

The standard vertical profile models developed during the TRMM era assumed that all precipitation-sized particles were spherical, due to the simplicity of computing the single-scattering properties of spherical particles. However, it is known that larger raindrops are better approximated by oblate spheroids, and ice-phase precipitation particles exhibit a variety of complicated particle geometries. The focus of our investigation will be to see if we can find reasonable parameterizations of ice- and mixed-phase precipitation particle size distributions and habits that produce bulk scattering properties which are consistent with simultaneous radar, radiometer, and *in situ* microphysics probe observations from the GPM field campaigns.

For each particle size in any prescribed particle size distribution, the mass (or density) of the particle, its structure or habit, and the meltwater fraction of the particle must be specified. Starting with purely ice-phase precipitation, we have examined the properties of both pristine crystals (plates, columns, dendrites) as well as aggregates of crystals. At right are photographs of a single dendrite and an aggregate of dendrites. Aggregate ice particles are particularly important because they tend to be the dominant particle type among particles of relatively large size, and they also produce high reflectivities at the onset of melting.

We have implemented a 3-D growth model for pristine crystals and a pseudo-gravitational collection model to create aggregate particles. The figures below the photographs show images of pristine ice crystals that we simulated using the growth model, and the various aggregates shown below the crystals are constructed from crystals of the same habit, but with different sizes and spatial orientations, that are sequentially collected. The constructed particles are filtered to represent different observed mass-size relations.

Using this method, roughly 6500 ice particles have been simulated, ranging from single pristine crystals to multi-crystal aggregates (sizes from 260 to 14,260 μm maximum dimension). Each ice particle is constructed on a 3D numerical grid, and the microwave single-scattering properties of each particle are computed using the discrete dipole approximation (DDA; see Draine and Flatau, 2003). In the DDA, a particle is represented by a grid of dipoles; each dipole interacts with an incoming electromagnetic wave as well as the scattered waves from all other dipoles in the particle. At lower right are simulations of the single-scattering parameters of the individual particles (blue) using DDA, as well as the parameters for spheres of the same mass and either variable density (solid green) or a constant density of 0.1 g cm^{-3} (dashed green), derived from Mie theory.

The backscatter efficiencies at the 13.6 and 35.5 GHz channels of the DPR are shown at right. Relative to the variable-density spheres, the constant density Mie spheres provide a better approximation to the aggregate particle efficiencies at these frequencies. However, note that at the 89 and 165.5 GHz channel frequencies of the GMI, the asymmetry parameters of the Mie spheres are consistently higher than the aggregate asymmetry parameters. This characteristic leads to an inability of Mie spheres to simultaneously fit radar and high-frequency radiometer data in field campaign tests (see right half of poster).

The single-scattering properties of multi-crystal aggregates with sizes greater than 14,260 μm (not shown), as well as melting aggregates, are now being calculated.

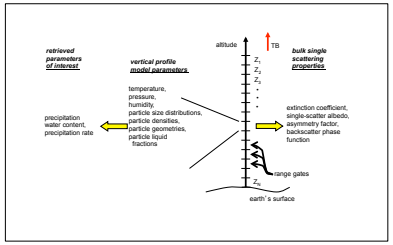

from Kenneth Libbrecht; snowcrystals.com

from Ron Stewart; McGill University

simulated crystals/aggregates and their single-scattering properties

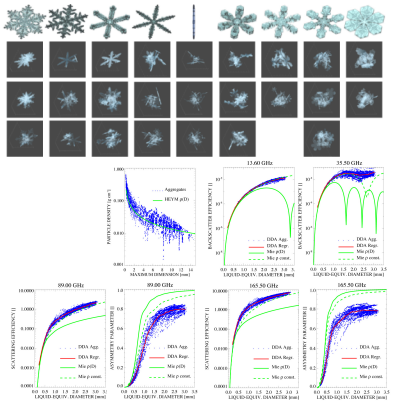

MC3E Observations for Testing

During the Midlatitude Continental Convective Clouds Experiment (MC3E), the ER-2 aircraft carried both the High-altitude Wind and Rain Profiling Radar (HIWRAP) and the Conical Scanning Millimeter-wave Imaging Radiometer (CoSMIR), which simultaneously viewed vertical columns of the atmosphere at nadir view. The HIWRAP radar operates at 14 GHz (Ku band) and 34 GHz (Ka band), while the CoSMIR senses upwelling microwave radiances from 50 to 183 GHz. The specific channels selected for HIWRAP and CoSMIR mimic the channels of the GPM DPR and GMI, respectively.

Also during MC3E, the University of North Dakota Citation aircraft provided *in situ* microphysics probe measurements of precipitation in underflights of the ER-2. These data have been analyzed to provide estimates of the size distributions of precipitation along portions of the ER-2 flight segments.

Finally, an enhanced sounding network operating during MC3E provided vertical profiles of temperature and humidity over a region encompassing the aircraft observations.

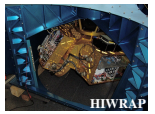

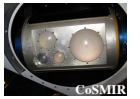

Consistency of Ice Particle Models with MC3E Observations

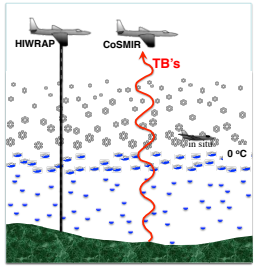

Our overall strategy is to use the field campaign observations to differentiate, to the greatest degree possible, the alternative models of simulated precipitation particles that might be considered for combined radar-radiometer algorithm applications in GPM. The figure at left illustrates the implementation of this strategy using MC3E data. The first step of the procedure is to select a particle scattering model for precipitation. Since the focus of the current testing is the scattering model for ice-phase precipitation, we specify either the spherical or aggregate ice particle models, previously described, to represent the ice phase. Standard spherical particle models for liquid and mixed-phase precipitation are also specified, and these remain fixed, regardless of the ice-phase particle model chosen.

Next, the dual-wavelength radar inversion method of Grecu et al. (2011) is applied to the Ku and Ka nadir-view reflectivity data from the HIWRAP, using one of the ice particle models to describe the single-scattering properties of those particles. The Grecu et al. (2011) algorithm is based upon a variational methodology that adjusts the vertical profile of precipitation size distribution intercepts such that forward-recursive precipitation size distributions estimates derived from the profile of Ku-band reflectivities are altered to be consistent with simultaneous Ka-band reflectivities and path-integrated attenuation estimates at Ku and Ka band. In these inversions, the bulk single-scattering properties of precipitation are represented by "scattering tables" that can be efficiently queried to find the median size and bulk attenuation of the precipitation, and the reflectivity of the precipitation at Ka band, given an estimate of the Ku-band attenuation-corrected reflectivity and precipitation size-distribution intercept, in addition to an assumed size-distribution shape factor.

Once a precipitation size distribution profile consistent with Ku/Ka band HIWRAP profiles is estimated, the same profile is used to simulate the upwelling radiaces (TB's) at the CoSMIR channel frequencies. This simulation requires data from the radiosondes to calculate the absorption of microwaves by atmospheric gases. Because the liquid and mixed-phase precipitation efficiently absorb upwelling microwave radiation, the upwelling microwave radiances at the top of the melting layer are not greatly sensitive to the details of the HIWRAP-retrieved precipitation, or assumptions regarding the electromagnetic properties of the precipitation, below the freezing level. Therefore, the variation of radiances observed by CoSMIR is primarily due to the concentration of ice-phase precipitation and the properties of the ice-phase precipitation particles. One test of a given ice precipitation particle model is, then, whether or not the retrieved ice-phase precipitation profiles consistent with the HIWRAP are also consistent with the observed CoSMIR brightness temperatures. Coincident *in situ* precipitation size distribution measurements from the underflying Citation provide independent validation of the size distribution parameters derived from the HIWRAP.

On 20 May 2011, both the ER-2 and Citation made flights into the stratiform precipitation region trailing an eastward-propagating squall line during MC3E. At right (upper left panel) is an ER-2 flight track segment displayed against the infrared cloud-top temperatures from GOES-East at the approximate time of the flight segment shown; also indicated are the locations of sounding stations that yielded the temperature profiles seen in the upper right panel. Below these panels are the vertical cross-sections of reflectivity from the HIWRAP at Ku & Ka bands, along the flight segment.

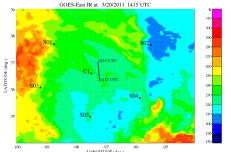

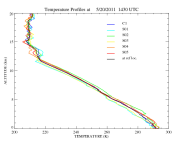

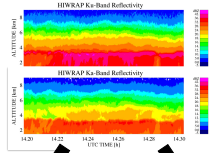

At right, below, the HIWRAP data are used to estimate the vertical cross-section of precipitation liquid-equivalent water contents using the spherical ice particle model (left column) and non-spherical, aggregate ice particle model (right column). In this demonstration, spherical particles with a constant density of 0.1 g cm^{-3} are employed, but particles of alternative densities, and size-dependent densities, were also tested. Note also that the precipitation size distribution shape factor and water vapor concentration are varied in the HIWRAP retrievals to account for uncertainties in those parameters; the mean estimated precipitation distributions are shown in the figures. From the precipitation distributions, upwelling radiances at the CoSMIR frequencies of 89 GHz (blue) and 165.5 GHz (red) are simulated using a delta-Eddington "Second" Approximation radiative transfer solution (next lower panels). The simulated radiances can be compared visually with the CoSMIR-observed radiances in the bottom panels at right.

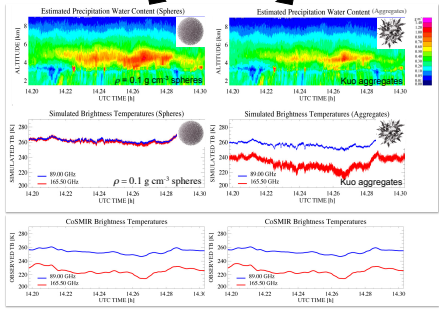

Note that the radiances simulated using the spherical ice precipitation particle model are systematically higher than the observed, particularly at 165.5 GHz. Variations in size distribution shape factor and water vapor cannot account for these discrepancies, nor can the choice of ice particle density (not shown). On the other hand, the HIWRAP retrievals and radiance simulations based on the aggregate ice particle model show reasonable consistency with the CoSMIR observations at both frequencies. Other flight legs on 20 May yielded similar results.